Nominally static frictional contacts under periodic loading

J.R.Barber[a]

[a]*Department of Mechanical Engineering, University of Michigan, Ann Arbor, MI 48109-2125, U.S.A.*

Abstract

We review recent developments in the response to periodic loading of elastic systems with frictional interfaces. The steady state can involve shakedown (no slip at any point), cyclic microslip leading to energy dissipation and possible fretting damage, or ratchetting (relative rigid-body motion accumulating during each cycle). Shakedown theorems can be established for systems in which the normal and tangential problems are uncoupled, but for coupled systems, the steady state depends on the initial conditions. In such cases the system 'memory' resides in the slip displacements at permanently stuck nodes. Analytical and asymptotic (continuum) methods for solving cyclic slip problems are also discussed.

Keywords: periodic loading; shakedown; friction

1. Introduction

Suppose two elastic bodies are pressed together by a normal force P and then subjected to a gradually increasing tangential force Q, as shown in Figure 1. This process was described in classical papers by Cattaneo (1938) and Mindlin (1949) for the case of Hertzian contact between bodies with quadratic surfaces. They found that as Q increases at constant P, regions of relative tangential displacement or *microslip* develop at the edges of the contact area.

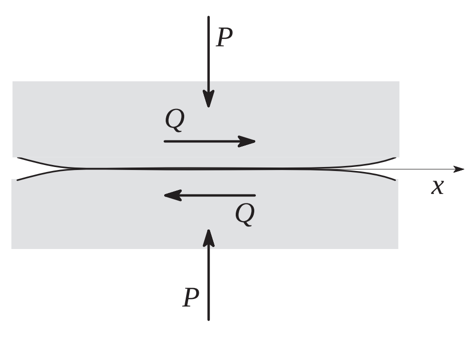

Figure 1: The Cattaneo-Mindlin problem.

*Corresponding author, jbarber@umich.edu

1.1. Microslip and gross slip

The microslip regions grow as the tangential force increases, until the entire contact area is slipping, at which point the bodies will slide over each other, if they posess an appropriate rigid-body degree of freedom. We shall refer to this latter state as *gross slip*. There are many important differences between gross slip and microslip. For example, the relative tangential displacements in a microslip region can be determined by integrating the relative tangential strains from the slip-stick boundary, and hence they are necessarily very small in most practical cases. By contrast, once gross slip commences, arbitrarily large relative displacements can occur. Also, the microslip surfaces remain permanently in contact, so any resulting wear particles may remain trapped at the interface and hence influence the contact problem. An important consequence of these observations is that friction laws determined experimentally under sliding conditions may not be appropriate to problems involving microslip.

1.2. Periodic loading, vibration, and fretting

Many engineering systems comprise nominally static contacting bodies subjected to forces that include a periodic component. This may be due to mechanical vibration, or to diurnal temperature variations, or to repetitive machine operating cycles. Typical applications include bolted joints and shrink fit assemblies, but other examples can be found ranging from tectonic plate contact to nanoscale systems. In the steady state, such systems will typically experience cyclic microslip, which implies that some energy is dissipated during each cycle. In a dynamic analysis, this will be reflected as (typically) hysteretic damping, which will influence the overall dynamic behaviour of the system. Indeed, it has been estimated that in many machines, the frictional energy dissipation at nominally static bolted joints is larger than that due to internal material damping. This energy dissipation also implies the occurrence of irreversible process in the microslip region, typically involving cyclic plasticity on the microscale or below. This in turn will eventually lead to the exhaustion of the material ductility, resulting in the detachment of wear particles (Goriacheva *et al.*, 2001), and the initiation and propagation of fretting fatigue cracks (Nowell *et al.*, 2006). Fretting fatigue in particular is of critical importance in the design of gas turbines with replaceable blades.

2. The Coulomb friction law

In this paper, we shall mostly restrict attention to the case where the contacting bodies are linearly elastic and microslip is governed by the classical friction law associated with the names of Amontons and Coulomb. Each point in the potential contact area is assumed to be in one of three states: stick, slip, or separation, in which the governing equations and inequalities are

$$\text{Stick:} \qquad w = 0\ ; \quad \dot{\boldsymbol{v}} = 0\ ; \quad p \geq 0\ ; \quad |\boldsymbol{q}| < fp \tag{1}$$

$$\text{Slip:} \qquad w = 0\ ; \quad |\dot{\boldsymbol{v}}| > 0\ ; \quad p \geq 0\ ; \quad \boldsymbol{q} = -\frac{fp\dot{\boldsymbol{v}}}{|\dot{\boldsymbol{v}}|} \tag{2}$$

$$\text{Separation:} \qquad w > 0\ ; \quad p = 0\ ; \quad \boldsymbol{q} = 0\ , \tag{3}$$

where f is the coefficient of friction, p is the contact pressure, $\boldsymbol{q}$ is the frictional (tangential) traction, w is the normal separation (gap), $\boldsymbol{v}$ is the relative tangential displacement (the slip displacement), and the dot indicates a time derivative.

2.1. The rate problem

With these conditions, we seek to determine the evolution of the displacement field $\boldsymbol{u}(x, y, z, t)$ in the elastic bodies in response to given initial conditions $\boldsymbol{u}(x, y, z, 0)$ and a known loading history $F(t)$. This in turn can be solved in principle if we can solve the so-called *rate problem* in which the displacement rate $\dot{\boldsymbol{u}}(x, y, z, t)$ is determined as a function of the instantaneous state $\boldsymbol{u}(x, y, z, t)$ and the time derivative of the loading $\dot{F}(t)$. Mathematically, this problem is very challenging, since in general it is not possible to prove that it has a unique solution. More progress has been made with the corresponding discrete problem in which contact is restricted to a finite set of nodes at which conditions (1–3) are imposed on the corresponding nodal values. In this case, existence and uniqueness can be established for the rate problem provided $f < f_{\rm cr}$, where the critical coefficient of friction $f_{\rm cr}$ can be determined from Klarbring's P-matrix condition (Klarbring, 1996).

From an engineering perspective, discrete models, notably those generated from the finite element method, are routinely assumed to give an acceptable approximation to the corresponding continuum problem, so one might expect that Klarbring's result will give us some insight into the physical behaviour of continuous systems. His criterion is very computationally intensive when there are large numbers of nodes, but estimates of $f_{\rm cr}$ from a relatively coarse model of the same system might be acceptable in many cases. For coefficients of friction $f > f_{\rm cr}$, various kinds of behaviour have been documented, including wedging (Hassani *et al.*, 2003, Hild, 2004), dynamically unstable solution branches (Ahn, 2010), and times at which the quasi-static solution requires a sudden jump to a new state (Martins *et al.*, 1992). In this paper, we shall restrict attention to problems for which $f < f_{\rm cr}$.

Broadly speaking, $f_{\rm cr}$ varies inversely with the degree of coupling between normal tractions and tangential displacements or *vice versa*. We shall discuss other consequences of this coupling in the following sections. Also we anticipate that $f_{\rm cr}$ will be related to the coefficient of friction needed to allow the system to become wedged — i.e. to remain in a state of stress under the influence of contact tractions, but with no external loads. However, no formal relation between the wedging problem and the rate problem has been established, except in particular cases (Barber and Hild, 2006).

2.2. The contact stiffness matrix

Consider a linear finite element discretization of a frictional contact problem in which there are M nodes in total, of which N are contact nodes. For a three-dimensional problem, the full model will have $3M$ degrees of freedom corresponding to the nodal displacement components, but the resulting equations for the $(M - N)$ non-contact nodes can be solved for the corresponding displacements, leaving a $3N \times 3N$ *contact stiffness matrix* connecting the contact displacements and the corresponding contact forces. This procedure is known as static reduction and methods for applying it are discussed by Thaitirarot *et al.*, (2014). The resulting model has the same form as that for a system of N blocks connected by springs and sliding against a corresponding set of obstacles. A simple two-node, two-dimensional system of this kind is illustrated in Figure 2.

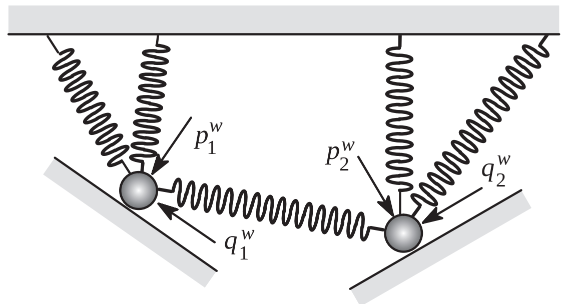

Figure 2: A two-node frictional elastic system.

We choose to make a further partition of the reduced stiffness matrix into components normal and tangential to the local interface, obtaining the elastic relation

$$\left\{ \begin{array}{c} \boldsymbol{q} \\ \boldsymbol{p} \end{array} \right\} = \left\{ \begin{array}{c} \boldsymbol{q}^w(t) \\ \boldsymbol{p}^w(t) \end{array} \right\} + \left[\begin{array}{cc} \boldsymbol{A} & \boldsymbol{B}^T \\ \boldsymbol{B} & \boldsymbol{C} \end{array} \right] \left\{ \begin{array}{c} \boldsymbol{v} \\ \boldsymbol{w} \end{array} \right\} , \tag{4}$$

where $p_i^w(t), \boldsymbol{q}_i^w(t)$ are the contact (nodal) forces that would be produced by the external loads if the nodes were all welded in contact at $\boldsymbol{v} = \boldsymbol{w} = \boldsymbol{0}$. Notice that in the three-dimensional problem, the tangential nodal force $\boldsymbol{q}_i$ is itself a 2-vector, since slip can occur in any direction in the contact plane, whereas in two dimensions both p_i and q_i are scalars. Most of the rest of this paper will be discussed in terms of the discrete model of equation (4).

2.3. Loading cycles

We consider the case where the external loading takes the form

$$\left\{ \begin{array}{c} \boldsymbol{q}^w(t) \\ \boldsymbol{p}^w(t) \end{array} \right\} = \left\{ \begin{array}{c} \boldsymbol{q}_0^w \\ \boldsymbol{p}_0^w \end{array} \right\} + \lambda \left\{ \begin{array}{c} \boldsymbol{q}_1^w(t) \\ \boldsymbol{p}_1^w(t) \end{array} \right\} , \tag{5}$$

where $\boldsymbol{q}_0^w, \boldsymbol{p}_0^w$ are time-independent mean loads, $\boldsymbol{q}_1^w(t), \boldsymbol{p}_1^w(t)$ are normalized periodic loads with zero mean value, and λ is a scalar load factor.

2.4. Analogies with plasticity

The Coulomb friction law has many similarities with plasticity in the absence of strain hardening. In the latter case, each point in the material remains elastic until a certain critical condition is reached [the failure surface] after which irreversible plastic strains accumulate while the stress state remains on the failure surface. Unloading is initially elastic, but the plastic strains remain and will generally lead to a state of residual stress after complete unloading. In the frictional problem, all nodes remain stuck until the inequality in (1) is violated, after which relative tangential displacements (slips) $\boldsymbol{v}_i$ accumulate whilst remaining on the 'failure surface' $|\boldsymbol{q}_i| = fp_i$. As in the plasticity problem, these slips will generally contribute to a state of residual stress.

2.5. *Shakedown*

In both cases, residual stresses are generally ‘favourable’ in the sense that they tend to reduce the liability for further plastic strain or frictional slip during subsequent periodic loading cycles. In some cases, a state of residual stress is developed sufficient to prevent all plastic deformation during subsequent cycles and this condition is known as *shakedown*. For elastic-plastic systems, Melan’s theorem (Melan, 1936) states that if any distribution of residual strain can be found sufficient to ensure shakedown, then the system will in fact shake down, though not necessarily to the state with the defined state of residual strain. In other words, ‘the system will shake down if it can’. For many years, tribologists assumed that a similar theorem applies to frictional slip (Churchman *et al.*, 2006), but Klarbring *et al.* (2007) showed that it applies if and only if the normal tractions have no effect on the tangential displacements, implying that the matrix $\boldsymbol{B}$ in equation (4) is null. Counter-examples, comprising loading scenarios in which shakedown depends on the initial conditions can always be found if $\boldsymbol{B} \neq \boldsymbol{0}$. Klarbring’s proof was extended to the corresponding continuum problem by Barber *et al.* (2008).

2.6. *Uncoupled systems*

Systems in which $\boldsymbol{B} = \boldsymbol{0}$ are known as *uncoupled*. In this case Klarbring’s P-matrix condition is satisfied for arbitrarily large friction coefficients, so the rate problem is always well posed (see §2.1).

The most important continuum problems in which the normal and tangential problems are uncoupled are (i) if the contact interface is a symmetry plane for the system, or (ii) if the two contacting bodies can be approximated as elastic half spaces making contact along a common plane interface, and Dundurs’ bimaterial constant $\beta = 0$ (Dundurs, 1969), or equivalently

$$\frac{(1-\nu_1)}{\mu_1} = \frac{(1-\nu_2)}{\mu_2} \; , \tag{6}$$

where ν_k, μ_k, $k = 1, 2$ are Poisson’s ratio and the shear modulus respectively for the materials of bodies 1,2. Finite element discretizations of these problems will lead to a system with $\boldsymbol{B} = \boldsymbol{0}$, provided the meshing near the contact plane is symmetric with respect to this plane.

2.7. *Cyclic slip*

If the system does not shake down under periodic loading, we anticipate that it will eventually tend to a steady periodic state. We can then identify a subset $\mathcal{T}$ of contact nodes such that for $i \in \mathcal{T}$, node i does not slip or separate at any time during the steady state. If the discrete system results from a finite element discretization of a continuum problem, the set $\mathcal{T}$ would define the *permanent stick zone*. Andersson *et al* (2014) have shown that for uncoupled discrete systems, $\mathcal{T}$ is independent of the initial conditions $\boldsymbol{v}(0)$, as are

- the status of any given node i (stick, slip or separation) at any time t;
- the frictional tractions $\boldsymbol{q}_i(t)$ for all nodes $i \neq \mathcal{T}$;
- the nodal slip velocities $\dot{\boldsymbol{v}}(t)$;
- the total frictional energy dissipation per cycle.

As in the shakedown case, the final steady state is not unique, since the nodal displacements $\boldsymbol{v}_i(t)$ are defined only to within a time-independent vector for all i and the tractions $\boldsymbol{q}_i(t)$ are not uniquely determined for $i \in \mathcal{T}$.

These results have important consequences for practical systems. For example, the effective damping of an uncoupled assembled structure will be independent of the assembly protocol, as will the pattern of fretting damage and the number of cycles to failure. The frictional Melan's theorem (Klarbring *et al.*, 2007) can be regarded as the special case of Andersson's theorem, in which all contact nodes belong to $\mathcal{T}$ and the frictional dissipation is zero.

3. Coupled systems

When the system is coupled ($\boldsymbol{B} \neq \boldsymbol{0}$) we must anticipate a possible dependence of the steady state on the initial conditions $\boldsymbol{v}(0)$. This implies that the system posesses some form of 'memory' and it is instructive to enquire where this memory might reside. Referring to equations (1–3), we notice that in each state we have one scalar and one vector equation for each node, but one of the equations for the 'stick' state defines only the time derivative $\dot{\boldsymbol{v}}_i(t)$, which leaves a degree of uncertainty in the actual value $\boldsymbol{v}_i(t)$. It is clear that if node i *never* slipped during the loading history, the value of $\boldsymbol{v}_i(t)$ would be equal to the initial value $\boldsymbol{v}_i(0)$, so in a sense, this node 'remembers' its initial value. More generally, this argument implies that the system memory resides in the slip displacements $\boldsymbol{v}_i(t)$ at nodes that are stuck at time t.

3.1. Ahn's diagram

Ahn *et al* (2008) showed how considerable insight into the behaviour of coupled systems can be obtained by tracking the motion of the point $P\{\boldsymbol{v}_1, \boldsymbol{v}_2, \boldsymbol{v}_3, ..., \boldsymbol{v}_N\}$ in $\boldsymbol{v}$-space. For the simple two-node system of Figure 2 (above), we have only two degrees of freedom v_1, v_2 and the progress of the system towards the steady state can be presented graphically.

If the two nodes are both in contact ($w_1 = w_2 = 0$), there are now four frictional inequalities

$$\begin{array}{rclll}
(A_{11} - fB_{11})v_1 + (A_{12} - fB_{12})v_2 & \leq & fp_1^w(t) - q_1^w(t) & \text{I} & (\dot{v}_1 < 0) \\
(A_{11} + fB_{11})v_1 + (A_{12} + fB_{12})v_2 & \geq & -fp_1^w(t) - q_1^w(t) & \text{II} & (\dot{v}_1 > 0) \\
(A_{21} - fB_{21})v_1 + (A_{22} - fB_{22})v_2 & \leq & fp_2^w(t) - q_2^w(t) & \text{III} & (\dot{v}_2 < 0) \\
(A_{21} + fB_{21})v_1 + (A_{22} + fB_{22})v_2 & \geq & -fp_2^w(t) - q_2^w(t) & \text{IV} & (\dot{v}_2 > 0)
\end{array} \quad (7)$$

governing incipient slip in each direction at the two nodes. The direction of incipient slip for each constraint is given in parentheses.

Each of these constraints excludes the region on one side of a straight line in $\boldsymbol{v}$-space, as illustrated in Figure 3, where P might instantaneously occupy any point in the central white quadrilateral. As the external loads $\boldsymbol{p}^w(t), \boldsymbol{q}^w(t)$ vary [for example, as in equation (5)], the constraint lines move, whilst preserving the same slope. Thus, for example, if the constraint IV in Figure 3 moves so as to exclude more space, it will 'push' P in the positive v_2-direction, representing 'forward' slip at node 2. More generally, the point P will only move when there is slip at one or both nodes, and in this state, P must lie on the appropriate boundary line(s). Notice that motion of P must be either horizontal or vertical [i.e. only one node slips at a time] unless two constraints are simultaneously active.

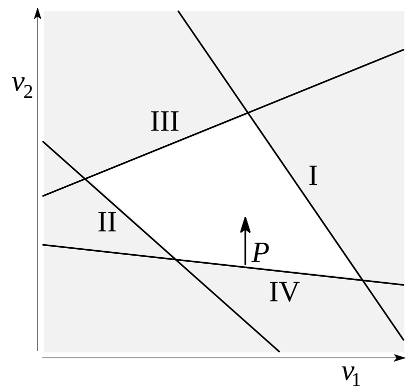

Figure 3: Evolution of the slip-displacement diagram. If constraint IV advances, it will push P in the direction $\dot{v}_2 > 0$, which represents forward slip at node 2.

During each period of loading, the constraints I, II, III, IV will move through the same sequence and we can define the corresponding extreme constraints $\mathrm{I^E}$, $\mathrm{II^E}$, etc. as the positions during the cycle that exclude the maximum amount of $\boldsymbol{v}$-space. In Figure 4, each constraint moves through the corresponding dark shaded region during each cycle, but there remains a 'safe shakedown region' which is never excluded by any of the constraints.

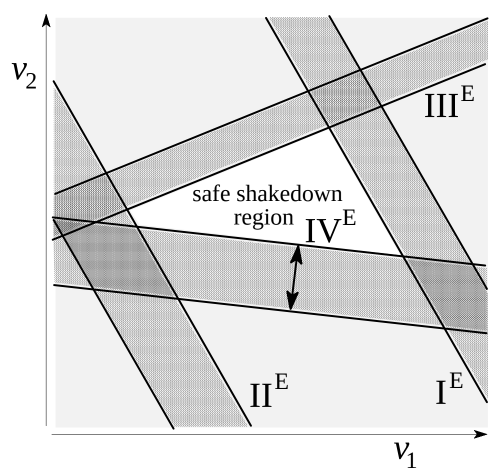

Figure 4: The extreme constraints $\mathrm{I^E}$, $\mathrm{II^E}$, $\mathrm{III^E}$, $\mathrm{IV^E}$, for a system exhibiting a safe shakedown region.

Ahn *et al.* (2008) showed that the two-node system will always shake down if the safe shakedown region is a quadrilateral, as shown in Figure 4, but shakedown will depend on initial conditions if it is triangular. The position of the extreme constarints for this latter case is illustrated in Figure 5. If the initial value of v_1 lies to the left of the safe triangle, the steady state of the system will involve oscillation between P_1 and P_2 as constraints III and IV advance and retreat (at different times during the cycle). Notice that the only constraint in (7) that can increase v_1 is II, and its extreme postion $\mathrm{II^E}$ in Figure 5 is too far to the left to allow P to reach the safe triangle. However, if the initial value of v_1 lies to the right of the shaded triangle, the final state is always shakedown.

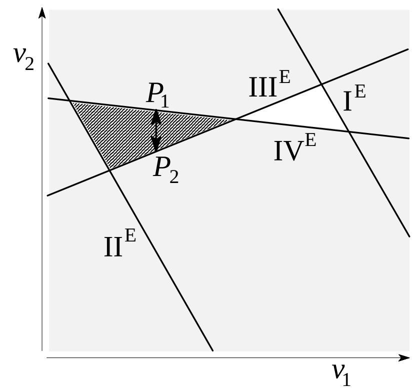

Figure 5: The white triangle defines a safe shakedown region, but whether it is reached depends on the initial value of v_1.

Notice that if $\boldsymbol{B} = \mathbf{0}$, the two lines defined by (7) for any given node are parallel, so the safe shakedown region is a parallelogram and hence always quadrilateral, confirming the results of the frictional Melan's theorem.

3.2. Multinode systems

Ahn's criterion can be extended to two-dimensional systems with any number of nodes, in which case the safe shakedown region is always reached if and only if all the $2N$ extreme constraints are active in defining this region. In the simple example of Figure 5, constraint II^{E} is not active in defining the shakedown region. More generally, if a particular extreme constraint is not active, we can identify points in the safe region for this constraint that lie outside all the active extreme constraints. If such a point is used as an initial condition, it follows that P will never reach the safe shakedown region.

3.3. Critical load factors

With the loading of equation (5), there will exist two critical load factors $\lambda_1 \leq \lambda_2$, such that for $\lambda < \lambda_1$, the system shakes down from all initial conditions, whereas for $\lambda > \lambda_2$ it cannot shake down. In the intermediate range $\lambda_1 < \lambda < \lambda_2$, whether shakedown occurs depends on the initial conditions. For $\lambda < \lambda_1$ the safe shakedown space comprises a hypervolume with $2N$ hyperplane facets, one corresponding to each extreme constraint, all of which are active. As $\lambda = \lambda_1$ is approached, one of these facets shrinks to a point, implying that the hyperplane corresponding to the constraint passes through an apex defined by the intersection of N other hyperplanes, one for each node. This is most easily visualized for the two node system, of Figure 5, where λ_1 is defined by the condition that the line II^{E} pass through the intersection of $\mathrm{III}^{\mathrm{E}}$ and IV^{E}.

For N nodes, intersections of this kind can be found by choosing any one of the two constraints for each of the N nodes, and then one further constraint [so that both constraints are included for this one node], replacing the inequalities by equalities, and solving the resulting set of $N + 1$ linear equations for the N displacements v_i and λ. There are $2^{N-1} \times N$ ways of choosing these equations, so we shall obtain a corresponding number of values of λ, the lowest of which defines λ_1. As with Klarbring's P-matrix criterion for the critical coefficient of friction, the problem becomes computationally prohibitive for large N, but we note that in a finite element discretization of a continuum problem, we might expect to get a reasonable estimate of λ_1 by using a relatively coarse model.

One of the remaining values of λ defined by this procedure will be λ_2, the value at which the safe shakedown region shrinks to a point. However, a more efficient approach to determining λ_2 is to define the maximum λ permitting permanent stick at all nodes as a function $\lambda(v_i)$ of the slip displacements v_i, and then choose the v_i to maximize λ (Björkman and Klarbring, 1987, Flicek *et al.*, 2015a).

3.4. Cyclic slip of coupled systems

If $\lambda > \lambda_2$, the steady state must be one of cyclic slip, but if the system is coupled, we anticipate that this state (and hence, for example, the steady-state frictional dissipation and damage) will depend on the initial conditions, at least as long as $\mathcal{T} \neq \emptyset$. We define the range in which this condition is satisfied as $\lambda < \lambda_3$, but notice that we must leave open the possibility that the set $\mathcal{T}$ is itself dependent on initial conditions.

For $\lambda > \lambda_3$, the permanent stick zone $\mathcal{T} = \emptyset$, so all nodes slip at least once during each cycle in the steady state. Recalling that the system memory is stored in the slip displacements at nodes that are instantaneously stuck, this implies the 'exchange' of memory between nodes during each cycle. We might expect this to lead to a gradual degradation of memory and hence to an asymptotic approach to a steady state.

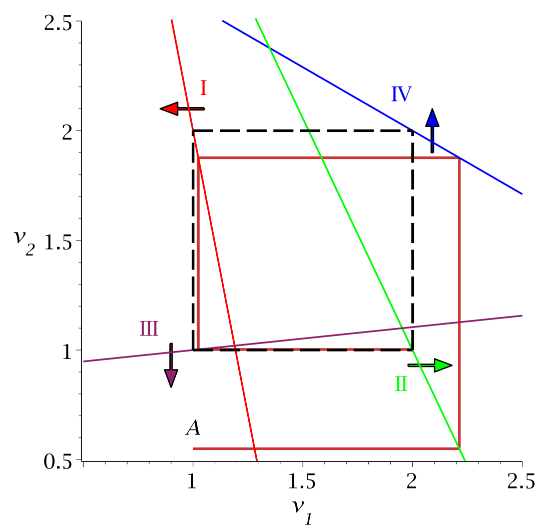

Figure 6: Convergence of the trajectory on a unique steady state.

We illustrate this process for the two-node system in Figure 6, where the initial condition is defined by point A. The external loads are defined such that the constraints advance and then recede in the sequence II→IV→I→III→II.... The extreme positions of these constraints are shown in the figure, from which we see that the point $P(v_1, v_2)$ will converge quite rapidly on a unique steady state, indicated by the dashed rectangle.

The evolution equations can be interpreted as defining an iterative algorithm to determine the state $P^{n+1}(\boldsymbol{v})$ as a function of the corresponding state $P^n(\boldsymbol{v})$ exactly one period earlier. In the complete periodic loading scenario, this iteration is performed repeatedly and trajectories such as the dashed rectangle in Figure 6 can then be seen as *attractors* for the iteration (Milnor, 1985). Andersson *et al.* (2013) have shown that with larger coefficients of friction and strong coupling, multiple attractors can be identified, and also some repellors — i.e. trajectories which strictly satisfy the steady-state iterative condition $P^{n+1}(\boldsymbol{v}) = P^n(\boldsymbol{v})$, but for which an arbitrarily small perturbation is sufficient to cause the system to diverge from the steady state, ultimately to be attracted by another steady state. Generally this behaviour requires larger coefficients of friction and strong coupling, but examples can be found without violating Klarbring's P-matrix condition.

3.5. Status of nodes in the permanent stick zone $\mathcal{T}$

If a particular node i slips during the steady state, it must experience periods of slip in both directions, since otherwise an unbounded slip would accumulate. However, during the transient approach to the steady state, we typically encounter nodes that slip only in a single direction during each cycle. In this case, the slips decrease with each successive cycle, generally approaching a summable geometric sequence at later stages of the process (Ahn and Barber, 2008). In the steady state, such nodes will experience 'incipient slip' at some point during each cycle in the steady state. In other words, the frictional inequality just reaches equality, but no slip actually occurs.

More generally, both cyclic slip and shakedown states usually involve a subset of nodes in the permanent stick zone $\mathcal{T}$ experiencing incipient slip at some point during the cycle. Pratt *et al.* (2010) have conjectured that the number of such nodes is reduced if the system experiences a transient (typically dynamic) overload condition. This is of relevance to nominally static collections of objects, such as masonry structures or granular media, which can sometimes be moved further from an incipient collapse state by one-time dynamic loading.

3.6. Summary

If the load factor λ is increased beyond λ_3, we shall eventually reach a value (λ_4) at which all the nodes slip simultaneously at least once during each cycle. When this happens, the equations (1–3) are sufficient to determine the instantaneous state uniquely, so no further dependence on initial conditions can occur. Thus, for a coupled system we anticipate the following ranges of λ:-

$0 < \lambda < \lambda_1$	Shakedown for all initial conditions.
$\lambda_1 < \lambda < \lambda_2$	Shakedown or cyclic slip depending on initial conditions.
$\lambda_2 < \lambda < \lambda_3$	Cyclic slip, but the steady state depends on initial conditions. At least some nodes must be permanently stuck.
$\lambda_3 < \lambda < \lambda_4$	Unique cyclic slip (or one of a few such states) approached asymptotically. The permanent stick zone $\mathcal{T} = \emptyset$.
$\lambda > \lambda_4$	Unique cyclic slip reached after one or two cycles. There is some time during each cycle when all nodes slip.

For uncoupled systems, $\lambda_2 = \lambda_1$ and in the range $\lambda_2 < \lambda < \lambda_3$, many features of the steady state are independent of initial conditions, as explained in §2.5.

If the bodies posess one or more degrees of freedom of rigid-body relative motion, the behaviour of the system is essentially unchanged for $\lambda < \lambda_3$, but is qualitatively different for $\lambda > \lambda_3$. In this case, sliding occurs as soon as λ_4 is reached, but in the range $\lambda_3 < \lambda < \lambda_4$ we can obtain behaviour analogous to 'ratchetting' in elastic plastic systems. Each node slips at least once during the cycle in the steady state, and the total nodal slip during a cycle is non-zero, leading to the accumulation of rigid-body motion. This can involve a rocking or walking motion (Mugadu *et a.*, 2004, Wetter and Popov, 2014, Ciavarella, 2015), or progressive slip and/or separation (Anscombe and Johnson, 1974). An application where this is of particular concern is the interference fit between the bushing and a conrod end, where accumulated relative rotation can cause oil holes to become misaligned and hence blocked (Antoni *et al.*, 2010).

4. Continuous systems

Most engineering contact problems are too intractable for analytical treatment, particularly when friction is involved, so we are more or less forced to use finite element or boundary element methods, which of course converts them to discrete problems. However, there are two important exceptions where significant analytical progress can be made with a continuum description:-

1. If the contact area is sufficiently small compared with the other linear dimensions of the bodies, so that these can be modelled as two elastic half spaces.
2. If slip is confined to a region at the edge of the contact area that is small compared with all other dimensions, including those of the contact area.

In continuum problems, the slip displacement $\boldsymbol{v}$ is a continuous function of position in the contact area. In two-dimensional problems, the derivatives $v'(s), w'(s)$ represent distributions of glide and climb dislocations respectively, where s is a coordinate defining position along the interface, and this permits the contact problem to be reduced to the solution of one or more integral equations if the appropriate dislocation solutions are known (Hills *et al.*, 1996).

4.1. Half-space models

Cattaneo (1938) and Mindlin (1949) showed that if the contacting bodies have quadratic profiles as in the Hertz contact problem (Johnson, 1985), the frictional (shear) tractions for the problem of Figure 1 in the uncoupled case ($\beta = 0$) are given by

$$q_x(x, y) = f\left[p(x, y) - p^*(x, y)\right] \ , \tag{8}$$

where $p(x, y)$ is the normal contact pressure and $p^*(x, y)$ is the contact pressure that would be developed at some smaller normal force P^* given by

$$P^* = P - \frac{Q_x}{f} \ . \tag{9}$$

Also, if the contact area at load P is defined as $\mathcal{A}(P)$, the instantaneous 'stick' area will be $\mathcal{A}_{\text{stick}} = \mathcal{A}(P^*)$, whilst the region $\mathcal{A}_{\text{slip}} = [\mathcal{A}(P) - \mathcal{A}(P^*)]$ slips. Ciavarella (1998a) and Jäger (1998) have since shown that this form of superposition is exact for all shapes of contacting bodies in the two dimensional case. Equations (8, 9) also define a good approximation in the general three-dimensional case (Ciavarella, 1998b), again subject to (6).

This method has been extended to general loading paths by Barber *et al.* (2011). During periods where

$$\dot{P} > 0 \quad \text{and} \quad \frac{d|Q|}{dP} < f \ , \tag{10}$$

the contact area increases and new contact is laid down in a state of full stick (Mindlin and Deresiewicz, 1953). At all other stages of the loading cycle, changes in the traction distribution can be expressed as a superposition of appropriate Ciavarella-Jäger distributions (8). For three-dimensional problems, this approach permits the relation between tangential displacement and tangential force and hence the dissipation per cycle to be expressed in terms of the incremental *normal* stiffness (Putigniano *et al.*, 2011).

4.1.1. Bulk stress

In practical applications, particularly those involving fretting fatigue, the contact problem is often complicated by the presence of a periodic bulk stress σ_1, σ_2 in one or both of the contacting bodies, as shown in Figure 7. If the tangential strains associated with these stresses are not equal, there will be a tendency for slip at the interface which interacts with that due to the tangential force Q.

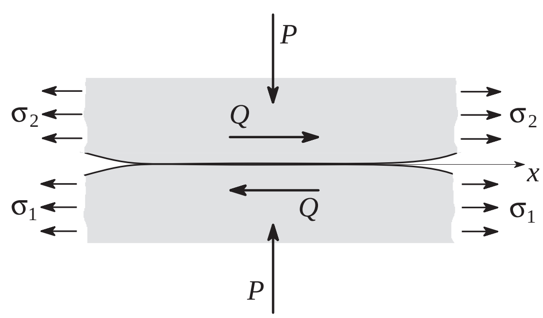

Figure 7: A contact problem involving bulk stress.

Ciavarella and Demelio (2001) have shown that for two-dimensional problems with relatively low levels of the bulk stress difference $|\sigma_1 - \sigma_2|$, the effect is merely to extend one of the two slip regions and reduce the other. Also, the Ciavarella-Jäger superposition (8) can be extended to this case for general geometries by defining $p^*(x, y)$ as the normal traction associated with a normal force P^* and a moment, or equivalently a normal force with a non-central line of action.

However, above some critical level of $|\sigma_1 - \sigma_2|$, slip will occur in opposite directions in the two slip zones, and a more complex solution strategy is required.

4.1.2. Incremental solution

An alternative approach to the solution of half-space problems with friction is to regard the instantaneous state as an appropriate integral of the incremental solution — i.e. of the change in traction distribution during an infinitesimal change of normal and tangential load. In the incremental problem, the contact area $\mathcal{A}$ and the stick area $\mathcal{A}_{\text{stick}}$ can be regarded as essentially unchanged, so the incremental problem in the two-dimensional case (for example) is defined by the boundary conditions

$$\frac{\partial u_z}{\partial x} = 0\ ; \quad x \in \mathcal{A} \tag{11}$$

$$\frac{\partial u_x}{\partial x} = 0\ ; \quad x \in \mathcal{A}_{\text{stick}} \tag{12}$$

$$q_x = \pm f p(x)\ ; \quad x \in \mathcal{A}_{\text{slip}}\ , \tag{13}$$

where u_z is the relative normal displacement and the sign in (13) depends on the direction of slip. In effect, the incremental problem is a continuum statement of the frictional rate problem.

Equations (11–13) define a 'flat punch' problem (possibly also including incremental bulk stresses) that can be solved in general for the two dimensional case, after which more general solutions can be constructed by integration (Hills *et al.*, 2011). This technique can also be used for coupled problems for the half space, where $\beta \neq 0$ and the corresponding incremental problem will involve both normal and shear tractions, even under purely normal incremental loading. Storåkers and Elaguine (2005) used this formulation to show that the stick zone $\mathcal{A}_{\text{stick}}$ during purely normal loading is a constant proportion of the total contact area $\mathcal{A}$ for contacting bodies of any shape, provided only that the contact area is a monotonic function of the normal load, a result that was previously established by Spence (1973) only for power-law profiles.

4.2. Slip near a corner

In systems subject to fretting fatigue, microslip is often confined to a region that is small compared with the extent of the contact area and the dimensions of the bodies, in which case results of some generality can be achieved using the asymptotic technique due to Williams (1952). In effect, the fields local to the corner are completely characterized by the generalized stress-intensity factors $K_{\text{I}}, K_{\text{II}}$, which are the multipliers on the first two terms in an asymptotic series for the stress field in powers of the distance r from the corner. Figure 8 shows the detail of a contact between a body with a right-angle corner and a plane surface.

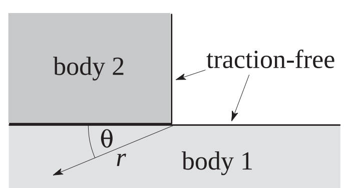

Figure 8: Indentation of an elastic half plane by a body with a right-angle corner.

For the case of similar materials, Churchman and Hills (2006) have shown that regardless of the far-field loading and macroscopic geometry, the corner must either stick or separate for coefficients of friction greater than 0.543. For lower coefficients of friction, a slip zone develops at the corner, whose length depends only on the ratio $K_{\text{II}}/K_{\text{I}}$. The application of these results to fretting fatigue problems is discussed by Flicek *et al.* (2015b).

Similar methods can be applied to determine the local perturbation in stress field and the extent of the slip zone due to a slightly rounded corner (Dini and Hills, 2004).

5. Conclusions

The behaviour of elastic systems with frictional interfaces is critically dependent on the extent of coupling between the normal tractions and the tangential (slip) displacements. If the system is uncoupled, a frictional equivalent of Melan's theorem applies, and above the shakedown limit, the frictional dissipation is independent of initial conditions. By contrast, coupled systems retain a memory of the initial conditions, which is stored in the slip displacements at permanently stuck nodes. Uncoupled problems that can be modelled as half spaces permit a fairly general analytical continuum solution, based on an extension of the Ciavarella-Jäger theorem.

References

Y. J. Ahn (2010), Discontinuity of quasi-static solution in the two-node Coulomb frictional system, *International Journal of Solids and Structures*, Vol. 47, pp. 2866–2871.

Y. J. Ahn, J. R. Barber (2008), Response of frictional receding contact problems to cyclic loading, *International Journal of Mechanical Sciences*, Vol. 50, pp. 1519–1525.

Y. J. Ahn, E. Bertocchi, J. R. Barber (2008), Shakedown of coupled two-dimensional discrete frictional systems, *Journal of the Mechanics and Physics of Solids*, Vol.56, pp. 3433–3440.

L-E. Andersson, J. R. Barber, Y-J. Ahn (2013), Attractors in frictional systems subjected to periodic loads, SIAM Journal of Applied Mathematics, Vol.73, pp. 1097–1116.

L.-E. Andersson, J. R. Barber, A. R. S. Ponter (2014), Existence and uniqueness of attractors in frictional systems with uncoupled tangential displacements and normal tractions, International Journal of Solids and Structures, Vol. 51, pp. 3710–3714.

H. Anscombe, K. L. Johnson (1974), Slip of a thin solid tire press-fitted on a wheel, *International Journal of Mechanical Sciences*, Vol. 16, pp. 329–334.

N. Antoni, Q. S. Nguyen, P. Ragot (2008), Slip-shakedown analysis of a system of circular beams in frictional contact, *International Journal of Solids and Structures*, Vol. 45, pp. 5189–5203.

J. R. Barber, P. Hild (2006), On wedged configurations with Coulomb friction, **in** Peter Wriggers and Udo Nackenhorst, **eds.**, *Analysis and Simulation of Contact Problems*, Springer-Verlag, Berlin, pp. 205–213.

J. R. Barber, A. Klarbring, M. Ciavarella (2008), Shakedown in frictional contact problems for the continuum, *Comptes Rendus Mecanique*, Vol. 336, pp. 34–41.

J. R. Barber, M. Davies, D. A. Hills (2011). Frictional elastic contact with periodic loading,*International Journal of Solids and Structures*, Vol. 48, pp. 2041–2047.

G. Björkman, A. Klarbring (1987). Shakedown and residual stresses in frictional systems. In: G. M. L. Gladwell, H. Ghonem, J. Kalousek, (Eds.), Contact Mechanics and Wear of Rail/Wheel Systems II: Proceedings of the 2nd International Symposium, pp. 27–39.

C. Cattaneo (1938), Sul contatto di due corpi elastici: distribuzione locale degli sforzi. *Rendiconti dell'Accademia Nazionale dei Lincei*, Vol. 27, pp. 342–348, 434–436, 474–478. (In Italian)

C. M. Churchman and D.A. Hills (2006), General results for complete contacts subject to oscillatory shear, *Journal of the Mechanics and Physics of Solids*, Vol. 54, pp. 1186–1205.

C. M. Churchman, A. M. Korsunsky, D. A. Hills (2006), The application of plasticity principles to friction. J. Strain Analysis Vol. 41, pp. 323–328.

M. Ciavarella, M. (1998a) The generalized Cattaneo partial slip plane contact problem. I-Theory, II-Examples. *Int.J.Solids Structures.* **35,** 2349–2378.

M. Ciavarella M, (1998b) Tangential loading of general 3D contacts. *ASME Journal of Applied Mechanics*, Vol. 65, 998–1003.

M. Ciavarella (2015), On the rocking and walking flat punch: Effect of elastic dissimilarity, *Tribology International*, Vol. 83, pp. 130–138.

M. Ciavarella and G. Demelio (2001), A review of analytical aspects of fretting fatigue, with extension to damage parameters, and application to dovetail joints, *International Journal of Solids and Structures*, Vol. 38, pp. 1791–1811.

D. Dini and D. A. Hills (2004), Bounded asymptotic solution for incomplete contacts in partial slip, *International Journal of Solids and Structures*, Vol. 41, pp. 7049–7062.

J. Dundurs (1969), Discussion on "Edge bonded dissimilar orthogonal elastic wedges under normal and shear loading", *ASME Journal of Applied Mechanics*, Vol. 36, pp.650–652.

R. C. Flicek, D. A. Hills, J. R. Barber, D. Dini (2015a), Determination of the shakedown limit for large, discrete frictional systems, *European Journal of Mechanics A/Solids*, Vol. 49, pp. 242–250.

R. C. Flicek, D. A. Hills, D. Dini (2015b), Sharp edged contacts subject to fretting: A description of corner behaviour, *International Journal of Fatigue*, Vol. 71, pp. 26–34.

I. G. Goriacheva, P. T. Rajeev, T. N. Farris (2001), Wear in partial slip contact, *ASME Journal of Tribology*, Vol. 123, pp. 848–856.

R. Hassani, P. Hild, I. R. Ionescu, N-D. Sakki (2003), A mixed finite element method and solution multiplicity for Coulomb frictional contact, *Computer Methods in Applied Mechanics and Engineering.*, Vol 192, pp. 4517–4531.

P. Hild (2004), Non-unique slipping in the coulomb friction model in two-dimensional linear elasticity, *Quarterly Journal of Mechanics and Applied Mathematics*, Vol. 57, pp. 225–235.

D. A. Hills, M. Davies, J. R. Barber (2011), An incremental formulation for half-plane contact problems subject to varying normal load, shear and tension, *Journal of Strain Analysis*, Vol. 46, pp. 436-443.

D. A. Hills, P. A. Kelly, D. N. Dai, A. M. Korsunsky (1996), *Solution of Crack Problems — The Distributed Dislocation Technique*. Kluwer Academic Publishers, Dordrecht, The Netherlands.

J. Jäger (1998), A new principle in contact mechanics, *ASME Journal of Tribology*, Vol. 120, pp. 677–684.

A. Klarbring (1999), Contact, friction, discrete mechanical structures and discrete frictional systems and mathematical programming. In: P. Wriggers and P. Panagiotopoulos (eds) New developments in contact problems. Wien: Springer, pp.55–100.

A. Klarbring, M. Ciavarella and J. R. Barber (2007), Shakedown in elastic contact problems with Coulomb friction, *International Journal of Solids and Structures*, Vol.44, pp.8355–8365.

J. A. C. Martins, M. D. P. Montiero Marques, F. Gastaldi and F. M. F. Simöes (1992), A two degree-of-freedom ‘quasistatic’ frictional contact problem with instantaneous jumps, Contact Mechanics International Symposium, Lausanne, Switzerland, pp. 217228.

E. Melan (1936), Theorie statisch unbestimmter Systeme aus ideal-plastichem Baustoff. Sitzungsber. d. Akad. d. Wiss., Wien 2A(145), pp. 195218

J. Milnor (1985), On the concept of attractor, *Communications of Mathematical Physics*, Vol. 99, pp. 177–195.

R. D. Mindlin (1949), Compliance of elastic bodies in contact, *ASME Journal of Applied Mechanics,* Vol.16, pp.259–268.

R. D. Mindlin and H. Deresiewicz (1953), Elastic spheres in contact under varying oblique forces, *ASME Journal of Applied Mechanics*, Vol. 75, pp.327–344.

A. Mugadu, A. Sackfield, D. A. Hills (2004), Analysis of a rocking and walking punch - Part I: Initial transient and steady state, *ASME Journal of Applied Mechanics*, Vol. 71, pp. 225–233.

D. Nowell, D. Dini, D. A. Hills (2006), Recent developments in the understanding of fretting fatigue, *Engineering Fracture Mechanics*, Vol. 73, pp.207–222.

E. Pratt, A. Leger, M. Jean (2010), About a stability conjecture concerning unilateral contact with friction, *Nonlinear Dynamics*, Vol. 59, pp. 73–94.

C. Putignano, M. Ciavarella, J. R. Barber (2011), Frictional energy dissipation in contact of nominally flat rough surfaces under harmonically varying loads, *Journal of the Mechanics and Physics of Solids*, Vol. 59 (2011), pp. 2442–2454.

D. A. Spence (1973), An eigenvalue problem for elastic contact with finite friction, *Proceedings of the Cambridge Philosophical Society,* Vol. 73, pp. 249–268.

B. Storåkers and D. Elaguine (2005), Hertz contact at finite friction and arbitrary profiles, *Journal of the Mechanics and Physics of Solids*, Vol. 53, pp. 1422–1447.

A. Thaitirarot, R. Flicek, D. A. Hills, J. R. Barber (2014), The use of static reduction in the solution of two-dimensional frictional contact problems, *Journal of Mechanical Engineering Science*, Vol. 228, pp. 1474–1487.

R. Wetter, V. L. Popov (2014), Influence of the alignment of load and oscillation on the frictional shakedown of an elastic rolling contact with Coulomb friction, *Physical Mesomechanics*, Vol. 17, pp. 265–273.

M. L. Williams (1952), Stress singularities from various boundary conditions in angular corners of plates in extension, *ASME Journal of Applied Mechanics,* Vol. 19, pp. 526–528.